How well does cholesteryl hemisuccinate mimic cholesterol in saturated phospholipid bilayers?

Waldemar Kulig,[1*] Joona Tynkkynen,[1] Matti Javanainen,[1] Moutusi Manna,[1] Tomasz Rog,[1] Ilpo Vattulainen,[1,2] and Pavel Jungwirth[3,1*]

[1] Department of Physics, Tampere University of Technology, P. O. Box 692, FI-33101 Tampere, Finland

[2] MEMPHYS-Center for Biomembrane Physics, University of Southern Denmark, Odense, Denmark

[3] Institute of Organic Chemistry and Biochemistry, Academy of Sciences of the Czech Republic, Flemingovo nám. 2, 16610 Prague 6, Czech Republic

[*] Corresponding authors: waldemar.kulig@tut.fi (WK) and pavel.jungwirth@uochb.cas.cz (PJ)

Abstract: Cholesteryl hemisuccinate is a detergent that is often used to replace cholesterol in crystallization of membrane proteins. Here we employ atomistic molecular dynamics simulations to characterize how well the properties of cholesteryl hemisuccinate actually match those of cholesterol in saturated protein-free lipid membranes. We show that the protonated form of cholesteryl hemisuccinate mimics many of the membrane properties of cholesterol quite well, while the deprotonated form of cholesteryl hemisuccinate is less convincing in this respect. Based on the results, we suggest that cholesteryl hemisuccinate in its protonated form is a quite faithful mimic of cholesterol for membrane protein crystallization, if specific cholesterol-protein interactions (not investigated here) are not playing a crucial role.

Keywords: molecular dynamics simulations, membrane elasticity, cholesterol, detergent

1. INTRODUCTION

Cholesterol (CHOL, Figure 1) is one of the key components in animal cell membranes. It influences numerous membrane properties, elasticity and fluidity being just a couple of the many examples, and it has a major role in a variety of physical processes taking place in membranes, such as lateral and transmembrane diffusion. Importantly, while cholesterol as well as its precursors, the naturally occurring sterol analogues (e.g. ergosterol), and also synthetic derivatives of cholesterol are all known to stabilize the structure of phospholipid bilayers, CHOL is among the most effective agents in this regard [1, 2].

The profound interest to understand the functions of cholesterol and its trafficking inside cells calls for methods to gauge its dynamics. This is not easy, though, since cholesterol is not naturally fluorescent. Thus, either fluorescent probes [3, 4] attached to cholesterol or fluorescent derivatives of cholesterol (dehydroergosterol, for instance) [5-8] have to be used instead. Often these molecules have properties quite close to those of cholesterol, thus they can be used to gain insight of the properties of cholesterol, too.

One of the most challenging topics in structural biology is the determination of 3D structures of membrane proteins. Cases where cholesterol has been observed to be part of the protein complex are quite common [9-14]. These proteins are thereby known as cholesterol-binding, and it is assumed that cholesterol has an important effect on protein function, such as an ability to promote thermal stability or to induce conformational changes in protein structure. However, the tricky aspect of these studies is that quite often it is not cholesterol that is used in protein 3D structure determination. Instead, one commonly uses cholesterol derivatives, such as cholesteryl hemisuccinate (CHS) [15-17].

CHS is a commercially available detergent widely used in integral membrane protein crystallization [16-19]. In order to maintain the native structure of membrane proteins, CHS should closely mimic the properties of cholesterol in native membranes [20]. Structurally the match between CHS and cholesterol is indeed quite good (Figure 1). It is also more soluble than cholesterol and therefore easier to use in biochemical studies of proteins, thus altogether it is understandable that CHS is commonly employed to replace cholesterol in unlocking the structures of membrane proteins, such as those in the GPCR family [15, 21-25].

The importance of CHS as a detergent is highlighted by its usefulness overall, as it has also been found to be an excellent membrane stabilizer in preparation of liposomes [26, 27]. However, the molecular mechanism by which CHS stabilizes membranes is not fully understood. It has been found experimentally to alter motions of acyl chains and the fluidity of cell membranes [28, 29]. Fluorescence polarization studies [30] have shown that CHS is approximately as effective as cholesterol in reducing the acyl chain mobility, hence altogether it seems to be a reasonably good

substitute for cholesterol. Furthermore, CHS is known to increase specific immunogenicity of tumor cells [31] and it can form pH-sensitive liposomes [32, 33] designed to undergo rapid destabilization in an acidic environment [34]. Such a condition occurs after cellular uptake of liposomes in endocytic vesicles. As a weak acid and as a liposome stabilizing agent, CHS is often used in liposomes in combination with other neutral lipids, both natural [28, 35] and synthetic [36]. pH-sensitive liposomes have been shown to be more efficient to deliver their contents to the cells than traditional ones [37]. In the case of gene delivery, CHS with other lipids coats the so-called polyplex-complex of DNA with polymers rather than encapsulating them inside the liposome [38]. CHS may also be used in combination with polymers coating liposomes in so-called stealth-pH sensitive liposomes, which due to the presence of neutral polymers (polyethylene glycol (PEG)) are not recognized by the immune system, thus extending their lifetime in circulation [39].

To our knowledge, there are no previous molecular simulations that would have considered the behavior of CHS in phospholipid bilayers, with only a single theoretical study of a pure CHS-containing bilayer being present in the literature [40]. The purpose of the present work is to bridge this gap and characterize the different effects of CHS vs. CHOL on phospholipid membranes. To this end, we performed extensive molecular dynamics (MD) simulations of mixed 1,2-dipalmitoyl-*sn*-glycero-3-phosphocholine (DPPC) bilayers containing 10 or 40 mol% of either CHS or its deprotonated form, denoted as CHSA. For comparison, analogous simulations with CHOL were also carried out. Key biophysical properties of these membranes, such as area per lipid, tilt angles of sterols, and deuterium order parameters were extracted from the CHS and CHSA simulations and compared to the corresponding values in cholesterol-containing DPPC bilayers. The results indicate that the protonated form of CHS mimics many of the membrane properties of cholesterol quite well, while the deprotonated form (CHSA) is less appropriate for this purpose. It seems plausible that CHS in its protonated form is a quite faithful mimic of cholesterol for membrane protein crystallization, if specific cholesterol-protein interactions are not important. In cases where specific interactions between cholesterol and the protein binding cholesterol are of a key relevance, our study cannot comment on the usefulness of CHS since the simulations we have carried out are protein free. Nonetheless, given that experiments have shown CHS to be a useful cholesterol-mimicking detergent, our simulation results support this view.

2. COMPUTATIONAL METHODS AND ANALYSIS

We performed atomistic MD simulations for seven different membrane systems. The first system (denoted as DPPC-0) was a bilayer composed of 128 molecules of DPPC. The next three systems contained 114 DPPC and 14 sterol molecules (CHOL, CHS, or CHSA), corresponding to a sterol concentration of 10 mol% (for molecular structures, see Figure 1). These systems are called CHOL-10, CHS-10, and CHSA-10, in respective order. The last three systems were composed of

76 DPPC and 52 sterol molecules (CHOL, CHS, or CHSA), corresponding to a sterol concentration of 40 mol% and denoted as CHOL-40, CHS-40, and CHSA-40, respectively. Table 1 presents the detailed compositions of all the systems investigated in this study.

Table 1. Summary of system compositions considered in this study. Shown here are the numbers of molecules/ions in each of the system.

System	DPPC	CHOL	CHS	CHSA	Na^+	Water
DPPC-0	128	-	-	-	-	6400
CHOL-10	114	14	-	-	-	6400
CHS-10	114	-	14	-	-	6400
CHSA-10	114	-	-	14	14	6386
CHOL-40	76	52	-	-	-	6400
CHS-40	76	-	52	-	-	6400
CHSA-40	76	-	-	52	52	6348

The initial structure of a DPPC bilayer was obtained by placing DPPC molecules on an 8 x 8 grid resulting in a bilayer comprised of two monolayers with an equal number of 64 lipids in each leaflet. Initial structures of the sterol-containing bilayers were obtained by randomly exchanging 14 or 52 DPPC molecules by the sterol molecules. Figure 2 shows the initial setup of the system, system after solvation, as well as the snapshot from the production run showing that the bilayer is stable during simulation.

Topologies of sterol molecules were built using parameters of existing molecular blocks from the all-atom OPLS (Optimized Parameters for Liquid Simulation) force field [41, 42]. Partial charges were also taken from the original all-atom OPLS force field. Force field parameters for DPPC were based on OPLS with partial charges for headgroup derived in a compatible manner with the OPLS procedure, and torsion angles in the headgroup were specifically derived for phospholipids. To avoid crystallization of hydrocarbons, also this part of the molecule was re-parameterized following the procedure described in ref [43]. The obtained model reproduces experimental data very well (see, e.g., the results section for the surface area per lipid molecule). Details of DPPC parameterization procedure will be published separately elsewhere. For water, we used the TIP3P model [44]. To neutralize bilayers containing CHSA, sodium ions described by standard OPLS parameters were added.

Temperature was kept at 323 K (which is above the phase transition temperature T_m = 314 K of DPPC [45]) using the Nosé-Hoover thermostat [46, 47] with a temperature coupling constant of 0.4 ps. Solvent molecules were coupled to the thermostat separately from other bilayer components. The pressure was kept constant with a semiisotropic scheme, meaning that the pressure in x and y directions (i.e., in the membrane plane) was coupled separately from the pressure in the z direction. The Parrinello-Rahman barostat [48, 49] was used to keep the pressure at 1 atm with a pressure coupling constant of 1ps and a compressibility of 4.5 x 10^{-5} bar^{-1}. Long-range electrostatic interactions beyond a non-bonded interaction cutoff of 1.0 nm were treated by the Particle Mesh Ewald scheme (PME) [50] with a Fourier spacing of 0.1 nm and a sixth order interpolation to the Ewald mesh. A long-range dispersion correction to the energy and pressure was added to maintain the compatibility with the parameterization procedure of the OPLS force field. The LINCS algorithm [51] was used to constrain all covalent bonds, allowing a time step of 2 fs. For water, the SETTLE method [52] was applied. Momentum of the system's center of the mass has been removed during simulation using standard algorithms implemented in the GROMACS software.

The systems were first energy minimized using the steepest descent algorithm, and then equilibrated in the constant temperature and pressure (NPT) ensemble until stable areas per molecule were obtained. After equilibration of at least 100 ns, production runs of 200 ns were performed. All simulations were performed with the GROMACS 4.6.x software package [53, 54].

Several measurable quantities were extracted from the simulation data. The area per molecule was calculated by dividing the total area of the simulation box in the x-y plane by the number of molecules in one leaflet. The membrane thickness was calculated as the average phosphate-to-phosphate (P-P) distance. The mean values of the deuterium order parameters ($|S_{CD}|$) [55] were calculated for the *sn*-1 and *sn*-2 acyl chains of DPPC, as well as for the sterol tails (C20-C22-C23-C24-C25, see Figure 1) using standard GROMACS scripts. The tilt angle of the sterol rings (defined as the angle between the C3-C17 vector (see Figure 1) and the bilayer normal), DPPC acyl tails (given as the angle between the C1-C16 (see Figure 1) vector and the bilayer normal), and sterol tails (defined as the angle between the C20-C25 vector and the bilayer normal), were calculated in order to characterize the orientation of sterols and lipids in the bilayer. For evaluation of the average number of contacts between different atomic groups, we used a cut-off distance of 4.5 Å (roughly corresponding to the minimum after the first maximum in the corresponding radial distribution functions). The contact is considered when the minimum distance between any pair of atoms from the respective groups is equal to or smaller than the cut-off distance. The volume (K_V) and surface (K_A) compressibility moduli of the system were determined using the following equations:

$$K_V \equiv -V\left(\frac{\partial P}{\partial V}\right)_T = \frac{Vk_BT}{\sigma_V^2}, \qquad K_A \equiv A\left(\frac{\partial P}{\partial A}\right)_T = \frac{Ak_BT}{\sigma_A^2} \quad (1),$$

where V is the volume of the simulation box, A is the total area of the membrane, P is the surface tension, T is the temperature, k_B is the Boltzmann constant, and σ_X^2 is the fluctuation of the quantity X.

All analyses in this study were performed on the data collected from production runs that were 200 ns long.

3. RESULTS AND DISCUSSION

All sterols decrease the area per molecule and increase membrane thickness, but the effects are the strongest with cholesterol

Area per molecule is one of the key variables characterizing membrane structure [55-58]. Its time evolution, free of any drifts, depicted in Figure 3 clearly shows that the area per molecule has converged in all systems already during the equilibration period (not shown in Figure 3). Sterols are found to decrease the area per lipid, leading to membrane condensation (see also the average areas given in Figure 4A). The effect of cholesterol is the strongest, followed by CHS and CHSA.

The reduction of the area per molecule due to the sterols is closely connected to an increase in the average membrane thickness. Figure 4B demonstrates that the effect of cholesterol on thickening the membrane is stronger than that of CHS and CHSA.

Sterols have distinct orientations coupled to their ordering ability

The tilt angle of a sterol characterizes the ability of the given sterol to order lipid acyl chains around it [59]. Figure 5A shows the distributions of sterol tilts in CHOL-10, CHS-10, and CHSA-10 systems. It is clear that the tilt of cholesterol rings is substantially smaller than the tilt of CHS or CHSA, and that the tilt angles of the last two compounds are almost the same. This picture is slightly changed at higher sterol concentrations (Figure 5B). Here, distributions of tilt angles become narrower and their maxima are shifted toward smaller angles. This correlates with the condensation effect described above – the higher the concentration of sterols, the more condensed the bilayer becomes, shifting the average tilt angles of sterols towards smaller values. Interestingly, this shift is not uniform for all the sterols. The biggest shift is present for CHS (~13°), followed by CHOL (~11.4°), and CHSA (~3.7°).

The tilt angle of a sterol ring describes the orientation of the sterol in the lipid bilayer but it does not say much about the sterol location. In order to elucidate the location of sterols in the lipid bilayers studied here, we calculated the mass density profiles of sterol oxygen atoms (O1 for

cholesterol, and carboxyl (O_C) and ester (O_E) oxygen atoms for CHS and CHSA, see Figure 1) and phosphatidylcholine phosphate oxygen atoms (O_P) along the normal of the bilayer. Figure 5 depicts the results (averaged over the two leaflets), where the profiles for the different systems have been aligned such that the O_P distributions in all bilayers overlap. This approach allows us to compare the location of each sterol inside the bilayer [60]. Figure 6 shows that the location of CHOL, CHS, and CHSA inside the membrane varies depending on the sterol type and its concentration. At the lower sterol concentration, the depth of the sterols inside the bilayer varies in the order CHS > CHOL > CHSA, while at the higher sterol concentration there is almost no difference between the three sterols. This effect reflects the ability of the sterols to condense the bilayer. Namely, at higher sterol concentrations the generic condensing effect of sterol rings becomes stronger than the individual differences between the sterols. The position of the carboxyl group (O_C atoms, broken lines in Figure 6) from CHS behaves in a similar manner. At the higher sterol concentration, there is no difference between CHS and CHSA, while at the lower concentration the -COO^- group of CHSA is on average closer to the membrane-water interface than the -COOH group of CHS.

Orientation of lipid acyl chains and sterol tails is coupled to local ordering around the molecules

Sterol rings induce the phosphatidylcholine acyl chains to straighten up, therefore causing them to order. This effect can be measured using various experimental techniques including NMR, EPR, or fluorescence spectroscopy [61-63]. Usually the order of lipid acyl chains is described in terms of the deuterium order parameter ($|S_{CD}|$); the higher the value of $|S_{CD}|$, the more ordered the bilayer is. Intriguingly, even relatively small changes in the chemical structures of the sterols studied here lead to considerable differences in the ordering of the DPPC bilayer, in agreement with previous observations for largely similar membrane systems [1, 64, 65]. Figure 7 clearly shows that cholesterol has the strongest ordering effect. For the cholesteryl hemisuccinates, CHS orders the acyl tails more than CHSA. The higher sterol concentration strengthens the ordering effect, but the differences between the sterols remain about the same.

Distributions of the tilt angles of the *sn*-1 and *sn*-2 chains of DPPC are shown in Figure 8. The presence of sterols decreases the tilt angle of the two DPPC tails as compared to a pure DPPC bilayer. This reduction is smaller in the bilayers containing 10 mol% of sterols, where the positions of the distributions' maxima in bilayers containing CHS and CHSA are almost the same as in the pure DPPC system. This effect is more visible in the bilayers whose sterol concentration is 40 mol%, where cholesterol reduces the tilt angle the most, followed by CHS and CHSA.

Figure 9 shows profiles for the deuterium order parameter along the sterol tail. Despite the fact that the tail is chemically identical in all sterols considered in this study (Figure 1), the $|S_{CD}|$ profiles differ substantially from each other: the order of CHS and CHSA tails is considerably lower than that along the cholesterol tail. The difference is significant already at the lower sterol concentration and becomes more pronounced in the bilayers with a higher concentration of

sterols. The effect can be explained by the ability of the sterols to condense the lipid bilayer, as described above.

The distributions of the sterol tails tilt angles are depicted in Figure 10, showing their preferable orientation in a DPPC bilayer. The cholesterol tail exhibits the lowest tilt, followed by that of CHS and CHSA. Interestingly, the maximum of the distribution in CHSA is practically unaffected by increasing sterol content, while the maxima for cholesterol and CHS are substantially (~10°) shifted toward smaller angles. This is likely due to the fact that the -COO^- group interacts more strongly with water molecules than the –COOH group, stabilizing thus the tilted conformations of CHSA.

Differences at the membrane-water interface are rather minor

To investigate the effect of the sterols on the membrane-water interface, we analyzed the average number of contacts between all molecules present in this region. Additionally, we considered the role of the sterols' hydrophilic groups (–OH, –COOH, –COO^-, and –OCO–) in the membrane-water interactions by calculating the average number of contacts between these groups and water. Results of this analysis are summarized in Table 2.

Table 2. Average number of contacts between different groups at the membrane-water interface. The hydrophilic group is –OH in CHOL, –COOH in CHS, and –COO^- in CHSA. Values for the ester group are given in the brackets. The results were normalized to the number of sterol-DPPC contacts.

	Sterol-water	**Sterol-DPPC**	**DPPC-water**	**Hydrophilic group-water**
CHOL-10	0.053	1	0.539	0.014
CHS-10	0.063	1	0.479	0.024 (0.004)
CHSA-10	0.153	1	0.536	0.050 (0.014)
CHOL-40	0.065	1	0.680	0.020
CHS-40	0.072	1	0.566	0.032 (0.003)
CHSA-40	0.171	1	0.701	0.057 (0.017)

The average number of contacts between a sterol and DPPC molecules seems to be almost independent of the sterol type, though it changes with sterol concentration. At high sterol concentration, the average number of sterol-DPPC contacts is smaller than at low sterol concentration. This may be surprising given that the presence of sterols condenses the membrane, shortening distances between their components, which in turn should increase the average number of contacts. However, at the higher sterol concentration, sterol-sterol interactions increase, leading to a decrease in the average number of sterol-DPPC contacts. This is not an issue for DPPC-water contacts, whose average number is almost constant and independent of the sterol type or its concentration.

Interestingly, the average number of sterol-water contacts does not depend on sterol concentration, though it varies substantially with sterol type. The number of sterol-water contacts increases as CHOL < CHS < CHSA, which can be explained by increasing hydrophilicity of functional groups present in each of these molecules. The hydroxyl group of CHOL is less hydrophilic than the protonated carboxyl group of CHS, which in turn is less hydrophilic than the deprotonated carboxyl group of CHSA. CHS and CHSA molecules also contain an ester group. Data gathered in Table 2 suggest that in CHSA the ester group is more hydrated (larger average number of ester group-water contacts) than in the case of CHS. This is likely connected to the higher hydrophilicity of the deprotonated vs. the protonated carboxylic group, allowing water to come closer to the ester group in the former case.

Membrane compressibility increases with increasing sterol concentration

Direct application of Eq. (1) gives the volume and surface compressibility moduli in the range of 14.3-18.1 kbar and 244.8-1653.0 dyn/cm, respectively. The calculated surface compressibility modulus (Table 3) for the pure DPPC bilayer corresponds nicely to the values observed in previous simulations [66]. It is rather clear that the surface compressibility modulus increases with increasing sterol concentration, which agrees with experimental observations for DMPC bilayers (where a fourfold increase was observed upon addition of 33-50 mol% of cholesterol) [67]. Here, the biggest increase is observed in the case of CHS, followed by CHOL and CHSA. The volume compressibility modulus (Table 3) seems to be almost independent of the sterol type, but it slightly increases with increasing sterol concentration.

Table 3. Volume and surface compressibility moduli calculated from the volume and area fluctuations using Eq. (1). The statistical errors are of the order of 20 %.

	K_A [dyn/cm]	K_V [kbar]
DPPC-0	244	15
CHOL-10	294	15
CHS-10	395	14
CHSA-10	254	15
CHOL-40	1550	18
CHS-40	1653	18
CHSA-40	1099	17

4. CONCLUSIONS

Using extensive MD simulations, we have characterized how cholesteryl hemisuccinate, one of the commonly used cholesterol-mimicking detergents, behaves in saturated lipid bilayers. We found that of the sterols considered in this work, cholesterol has the largest effect as a membrane-ordering agent. It is well known in the field that the strong ordering capacity of cholesterol has several implications in terms of slowing down lateral diffusion, changing the distribution of free volume inside a saturated lipid bilayer, and reducing membrane elasticity [55, 68]. As cholesteryl hemisuccinate (in particular its protonated form) has a comparable ordering effect on a DPPC bilayer, it is justified to assume that many of these cholesterol-induced effects on membrane properties hold for protonated cholesteryl hemisuccinate, to a considerable extent, too. The deprotonated form of cholesteryl hemisuccinate is a different matter, since its ordering effect on the DPPC bilayer was in this work found to be significantly weaker compared to its protonated form and cholesterol. As far as membrane protein crystallization protocols are concerned, our results suggest that cholesteryl hemisuccinate in its protonated form is a rather faithful mimic of cholesterol, if the purpose is to use it for creating a cholesterol-rich-like membrane environment that would stabilize the structure of membrane proteins under crystallization. However, this view holds only if the purpose of cholesteryl hemisuccinate were to adjust membrane elasticity, perhaps also the transmembrane lateral stress profile around the given protein, with no intention to include effects arising from specific cholesterol-protein interactions. If specific interactions are important, as is often the case with cholesterol-binding membrane proteins which have a specific binding pocket for cholesterol, then the situation is more complex and cannot be clarified by the results of this work, which does not include the protein explicitly. Nonetheless, experiments have shown that cholesteryl hemisuccinate is a useful detergent, mimicking cholesterol, and our simulation results support this view for its protonated form.

ACKNOWLEDGMENTS

We thank the Academy of Finland for support (the Finland Distinguished Professor (FiDiPro) program, and Center of Excellence funding). PJ thanks the Czech Science Foundation (grant P208/12/G016) and acknowledges the Academy of Sciences for the Praemium Academie award. IV thanks the European Research Council (Advanced Grant CROWDED-PRO-LIPIDS). CSC — IT Centre for Science (Espoo, Finland) is acknowledged for computational resources.

REFERENCES

[1] T Rog, M Pasenkiewicz-Gierula, I Vattulainen, M Karttunen (2009) Biochimica Et Biophysica Acta-Biomembranes 1788: 97. Doi:10.1016/j.bbamem.2008.08.022
[2] H Ohvo-Rekila, B Ramstedt, P Leppimaki, JP Slotte (2002) Progress in Lipid Research 41: 66. Doi:10.1016/s0163-7827(01)00020-0
[3] M Holtta-Vuori, RL Uronen, J Repakova, et al. (2008) Traffic 9: 1839. Doi:10.1111/j.1600-0854.2008.00801.x
[4] ZG Li, E Mintzer, R Bittman (2006) Journal of Organic Chemistry 71: 1718. Doi:10.1021/jo052029x
[5] FR Maxfield, D Wustner (2012) in DiPaolo G, Wenk MR (eds)Lipids, Vol 108Elsevier Academic Press Inc, San Diego
[6] JR Robalo, A do Canto, AJP Carvalho, JPP Ramalho, LMS Loura (2013) Journal of Physical Chemistry B 117: 5806. Doi:10.1021/jp312026u
[7] F Schroeder (1984) Progress in Lipid Research 23: 97. Doi:10.1016/0163-7827(84)90009-2
[8] D Wustner (2007) Chemistry and Physics of Lipids 146: 1. Doi:10.1016/j.chemphyslip.2006.12.004
[9] W Liu, E Chun, AA Thompson, et al. (2012) Science 337: 232. Doi:10.1126/science.1219218
[10] V Cherezov, DM Rosenbaum, MA Hanson, et al. (2007) Science 318: 1258. Doi:10.1126/science.1150577
[11] JP Morth, BP Pedersen, MS Toustrup-Jensen, et al. (2007) Nature 450: 1043. Doi:10.1038/nature06419
[12] M Laursen, L Yatime, P Nissen, NU Fedosova (2013) Proceedings of the National Academy of Sciences of the United States of America 110: 10958. Doi:10.1073/pnas.1222308110
[13] HJ Kwon, L Abi-Mosleh, ML Wang, et al. (2009) Cell 137: 1213. Doi:10.1016/j.cell.2009.03.049
[14] MB Lascombe, M Ponchet, P Venard, ML Milat, JP Blein, T Prange (2002) Acta Crystallographica Section D-Biological Crystallography 58: 1442. Doi:10.1107/s0907444902011745
[15] M Zocher, C Zhang, SGF Rasmussen, BK Kobilka, DJ Muller (2012) Proceedings of the National Academy of Sciences of the United States of America 109: E3463. Doi:10.1073/pnas.1210373109
[16] JA Christopher, J Brown, AS Dore, et al. (2013) Journal of Medicinal Chemistry 56: 3446. Doi:10.1021/jm400140q
[17] T Warne, R Moukhametzianov, JG Baker, et al. (2011) Nature 469: 241. Doi:10.1038/nature09746
[18] CA Shintre, ACW Pike, Q Li, et al. (2013) Proceedings of the National Academy of Sciences of the United States of America 110: 9710. Doi:10.1073/pnas.1217042110
[19] MA Hanson, V Cherezov, MT Griffith, et al. (2008) Structure 16: 897. Doi:10.1016/j.str.2008.05.001
[20] AM Seddon, P Curnow, PJ Booth (2004) Biochimica Et Biophysica Acta-Biomembranes 1666: 105. Doi:10.1016/j.bbamem.2004.04.011

[21] MA O'Malley, ME Helgeson, NJ Wagner, AS Robinson (2011) Biophysical Journal 100: L11. Doi:10.1016/j.bpj.2010.12.3698
[22] MA O'Malley, ME Helgeson, NJ Wagner, AS Robinson (2011) Biophysical Journal 101: 1938. Doi:10.1016/j.bpj.2011.09.018
[23] AA Thompson, JJ Liu, E Chun, et al. (2011) Methods 55: 310. Doi:10.1016/j.ymeth.2011.10.011
[24] K Vukoti, T Kimura, L Macke, K Gawrisch, A Yeliseev (2012) Plos One 7: 19. Doi:10.1371/journal.pone.0046290
[25] J Oates, B Faust, H Attrill, P Harding, M Orwick, A Watts (2012) Biochimica Et Biophysica Acta-Biomembranes 1818: 2228. Doi:10.1016/j.bbamem.2012.04.010
[26] GJ Zhang, HW Liu, L Yang, YG Zhong, YZ Zheng (2000) Journal of Membrane Biology 175: 53. Doi:10.1007/s002320001054
[27] WX Ding, XR Qi, P Li, Y Maitani, T Nagai (2005) International Journal of Pharmaceutics 300: 38. Doi:10.1016/j.ijpharm.2005.05.005
[28] MZ Lai, N Duzgunes, FC Szoka (1985) Biochemistry 24: 1646. Doi:10.1021/bi00328a012
[29] D Dumas, S Muller, F Gouin, F Baros, ML Viriot, JF Stoltz (1997) Archives of Biochemistry and Biophysics 341: 34. Doi:10.1006/abbi.1997.9936
[30] JB Massey (1998) Biochimica Et Biophysica Acta-Biomembranes 1415: 193. Doi:10.1016/s0005-2736(98)00194-1
[31] YG Skornick, GH Rong, WF Sindelar, et al. (1986) Cancer 58: 650. Doi:10.1002/1097-0142(19860801)58:3<650::aid-cncr2820580309>3.0.co;2-3
[32] IM Hafez, PR Cullis (2000) Biochimica Et Biophysica Acta-Biomembranes 1463: 107. Doi:10.1016/s0005-2736(99)00186-8
[33] S Simoes, JN Moreira, C Fonseca, N Duzgunes, MCP de Lima (2004) Advanced Drug Delivery Reviews 56: 947. Doi:10.1016/j.addr.2003.10.038
[34] RM Straubinger (1993) Methods in Enzymology 221: 361. Doi:10.1016/0076-6879(93)21030-c
[35] J Connor, MB Yatvin, L Huang (1984) Proceedings of the National Academy of Sciences of the United States of America-Biological Sciences 81: 1715. Doi:10.1073/pnas.81.6.1715
[36] M Carafa, L Di Marzio, C Marianecci, et al. (2006) European Journal of Pharmaceutical Sciences 28: 385. Doi:10.1016/j.ejps.2006.04.009
[37] N Skalko-Basnet, M Tohda, H Watanabe (2002) Biological & Pharmaceutical Bulletin 25: 1583. Doi:10.1248/bpb.25.1583
[38] J Lehtinen, Z Hyvonen, A Subrizi, H Bunjes, A Urtti (2008) Journal of Controlled Release 131: 145. Doi:10.1016/j.jconrel.2008.07.018
[39] TM Allen (1994) Trends in Pharmacological Sciences 15: 215. Doi:10.1016/0165-6147(94)90314-x
[40] B Klasczyk, S Panzner, R Lipowsky, V Knecht (2010) Journal of Physical Chemistry B 114: 14941. Doi:10.1021/jp1043943
[41] WL Jorgensen, J Tiradorives (1988) Journal of the American Chemical Society 110: 1657. Doi:10.1021/ja00214a001
[42] J Chandrasekhar, M Saunders, WL Jorgensen (2001) Journal of Computational Chemistry 22: 1646. Doi:10.1002/jcc.1120
[43] SWI Siu, K Pluhackova, RA Bockmann (2012) Journal of Chemical Theory and Computation 8: 1459. Doi:10.1021/ct200908r
[44] WL Jorgensen, J Chandrasekhar, JD Madura, RW Impey, ML Klein (1983) Journal of Chemical Physics 79: 926. Doi:10.1063/1.445869
[45] MR Vist, JH Davis (1990) Biochemistry 29: 451. Doi:10.1021/bi00454a021
[46] S Nose (1984) Molecular Physics 52: 255. Doi:10.1080/00268978400101201
[47] WG Hoover (1985) Physical Review A 31: 1695. Doi:10.1103/PhysRevA.31.1695
[48] M Parrinello, A Rahman (1981) Journal of Applied Physics 52: 7182. Doi:10.1063/1.328693
[49] S Nose, ML Klein (1983) Molecular Physics 50: 1055. Doi:10.1080/00268978300102851

[50] U Essmann, L Perera, ML Berkowitz, T Darden, H Lee, LG Pedersen (1995) Journal of Chemical Physics 103: 8577. Doi:10.1063/1.470117
[51] B Hess, H Bekker, HJC Berendsen, J Fraaije (1997) Journal of Computational Chemistry 18: 1463. Doi:10.1002/(sici)1096-987x(199709)18:12<1463::aid-jcc4>3.0.co;2-h
[52] S Miyamoto, PA Kollman (1992) Journal of Computational Chemistry 13: 952. Doi:10.1002/jcc.540130805
[53] E Lindahl, B Hess, D van der Spoel (2001) Journal of Molecular Modeling 7: 306.
[54] F Wennmohs, M Schindler (2005) Journal of Computational Chemistry 26: 283. Doi:10.1002/jcc.20163
[55] E Falck, M Patra, M Karttunen, MT Hyvonen, I Vattulainen (2004) Biophysical Journal 87: 1076. Doi:10.1529/biophysj.104.041368
[56] O Edholm, JF Nagle (2005) Biophysical Journal 89: 1827. Doi:10.1529/biophysj.105.064329
[57] C Hofsass, E Lindahl, O Edholm (2003) Biophysical Journal 84: 2192. Doi:10.1016/s0006-3495(03)75025-5
[58] SW Chiu, E Jakobsson, RJ Mashl, HL Scott (2002) Biophysical Journal 83: 1842.
[59] J Aittoniemi, T Rog, P Niemela, M Pasenkiewicz-Gierula, M Karttunen, I Vattulainen (2006) Journal of Physical Chemistry B 110: 25562. Doi:10.1021/jp064931u
[60] T Rog, M Pasenkiewicz-Gierula (2003) Biophysical Journal 84: 1818.
[61] E Oldfield, M Meadows, D Rice, R Jacobs (1978) Biochemistry 17: 2727. Doi:10.1021/bi00607a006
[62] JA Urbina, S Pekerar, HB Le, J Patterson, B Montez, E Oldfield (1995) Biochimica Et Biophysica Acta-Biomembranes 1238: 163. Doi:10.1016/0005-2736(95)00117-l
[63] R Jacobs, E Oldfield (1979) Biochemistry 18: 3280. Doi:10.1021/bi00582a013
[64] OHS Ollila, T Rog, M Karttunen, I Vattulainen (2007) Journal of Structural Biology 159: 311. Doi:10.1016/j.jsb.2007.01.012
[65] S Poyry, T Rog, M Karttunen, I Vattulainen (2008) Journal of Physical Chemistry B 112: 2922. Doi:10.1021/jp7100495
[66] E Lindahl, O Edholm (2000) Biophysical Journal 79: 426.
[67] D Needham, TJ McIntosh, E Evans (1988) Biochemistry 27: 4668. Doi:10.1021/bi00413a013
[68] E Falck, M Patra, M Karttunen, MT Hyvonen, I Vattulainen (2004) Journal of Chemical Physics 121: 12676. Doi:10.1063/1.1824033

FIGURE CAPTIONS

Figure 1. Chemical structures of DPPC, CHOL, CHS, and CHSA molecules with the carbon numbering scheme used in this study.

Figure 2. Molecular graphics view of the system (CHOL-10) showing the initial setup as well as the end of the simulation. Cholesterol molecules are depicted in green, while DPPC molecules are shown in red.

Figure 3. Area per molecule as a function of time, showing the production run (200 ns) of the simulations.

Figure 4. Average areas per molecule (A) and membrane thickness (B). Error bars were calculated as a RMSD (root mean square deviation) of the data.

Figure 5. Distribution of the tilt angles for the sterol rings (CHOL – red, CHS – green, and CHSA – blue).

Figure 6. Partial mass density profiles of a few specific sterol oxygen atoms along bilayer normal. Profiles have been shifted such that the distributions of the phosphate oxygen atoms in phosphatidylcholine headgroups overlap. Here, membrane depth = 0 corresponds to membrane center and only half of the membrane is shown to clarify the presentation. Results are given for the following molecular units: CHOL O1 atom (red, full line), CHS O_E atoms (green, full line), CHSA O_E atoms (blue, full line), CHS O_C atoms (green, dashed line), CHSA O_C atoms (blue, dashed line). For the atoms referred to, see Figure 1.

Figure 7. Deuterium order parameter ($|S_{CD}|$) profiles calculated for (A, C) the *sn*-1 and (B, D) *sn*-2 tails. Panels A and B correspond to 10 mol% sterol concentration, while panels C and D give the data for 40 mol%. Small carbon numbers correspond to those close to the glycerol group, while largest one is the terminal carbon. Colors are as follows: pure DPPC bilayer (black), CHOL (red), CHS (green), and CHSA (blue).

Figure 8. Distributions of the tilt angles of (A, C) the *sn*-1 and (B, D) *sn*-2 tails of DPPC. Panels A and B panel correspond to 10 mol% sterol concentration, while panels C and D show the data for 40 mol% sterol concentration. The color code is as follows: pure DPPC bilayer (black), CHOL (red), CHS (green), and CHSA (blue).

Figure 9. Deuterium order parameter ($|S_{CD}|$) profiles calculated for sterol tails. Panel A corresponds to 10 mol% sterol concentration, while panel B shows the data for 40% sterol content: CHOL (red), CHS (green), and CHSA (blue).

Figure 10. Distributions of the sterol tails' tilt angle. Panel A is for 10 mol% sterol concentration, and panel B for 40 mol%: CHOL (red), CHS (green), and CHSA (blue).

FIGURES

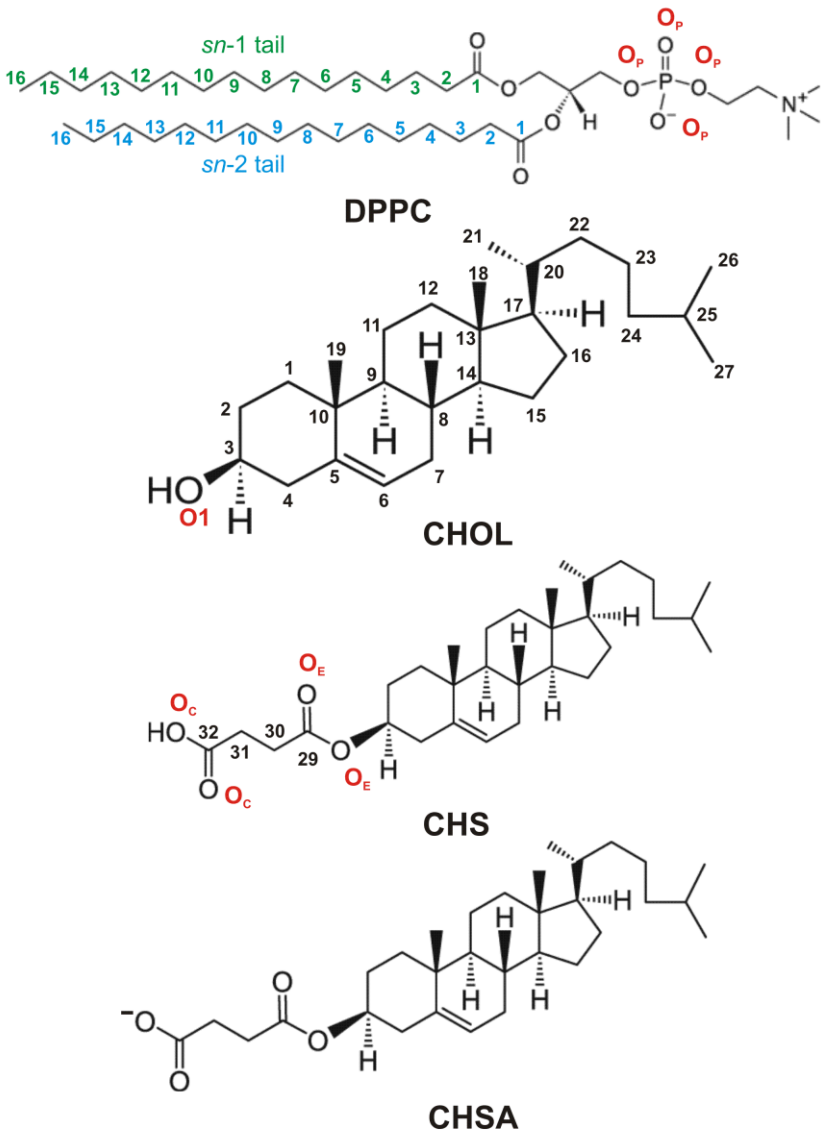

Figure 1.

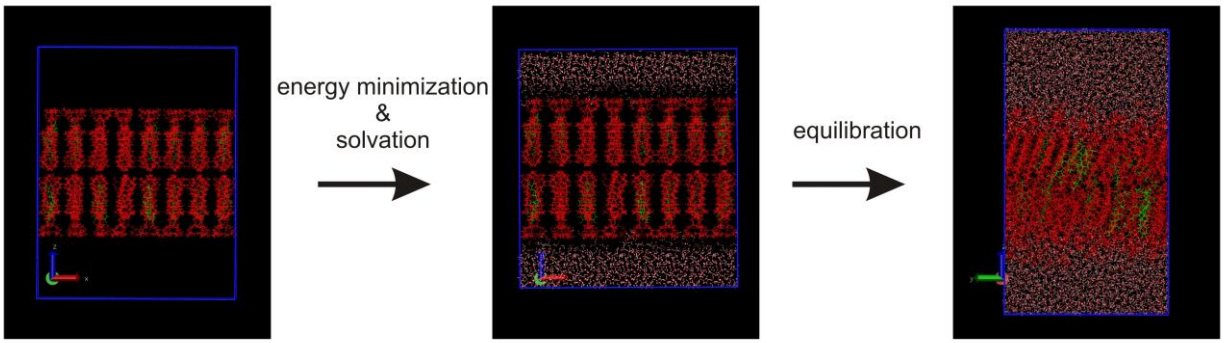

Figure 2.

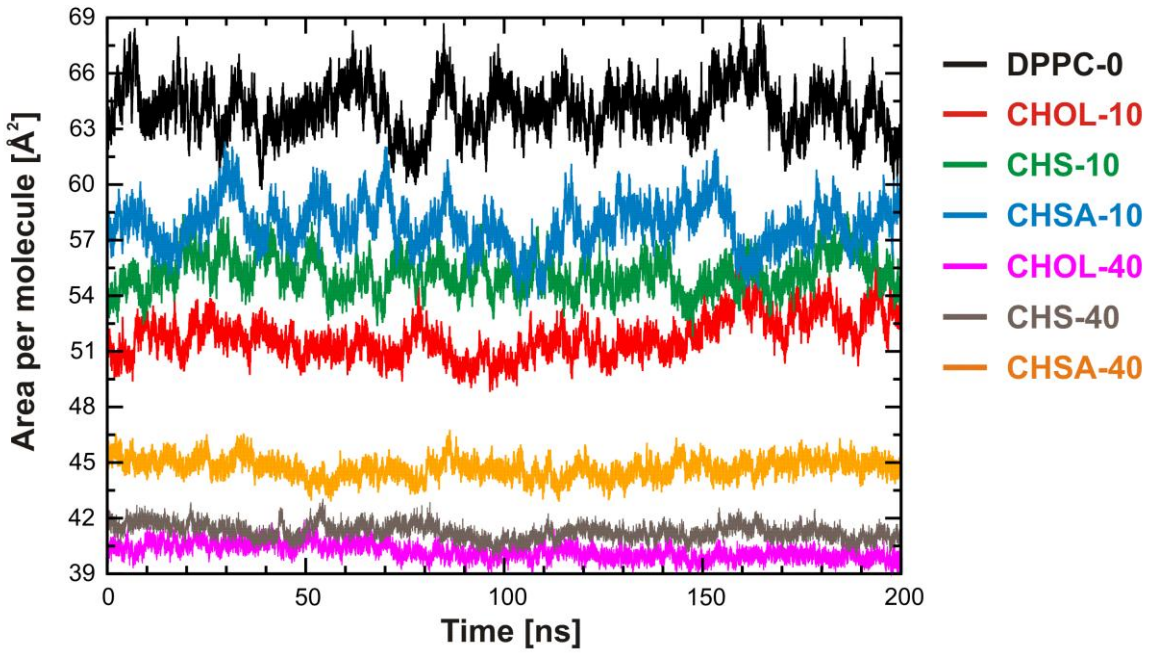
Area per molecule [Å²]
69
66
63
60
57
54
51
48
45
42
39
0
50
100
150
200
Time [ns]
DPPC-0
CHOL-10
CHS-10
CHSA-10
CHOL-40
CHS-40
CHSA-40

Figure 3.

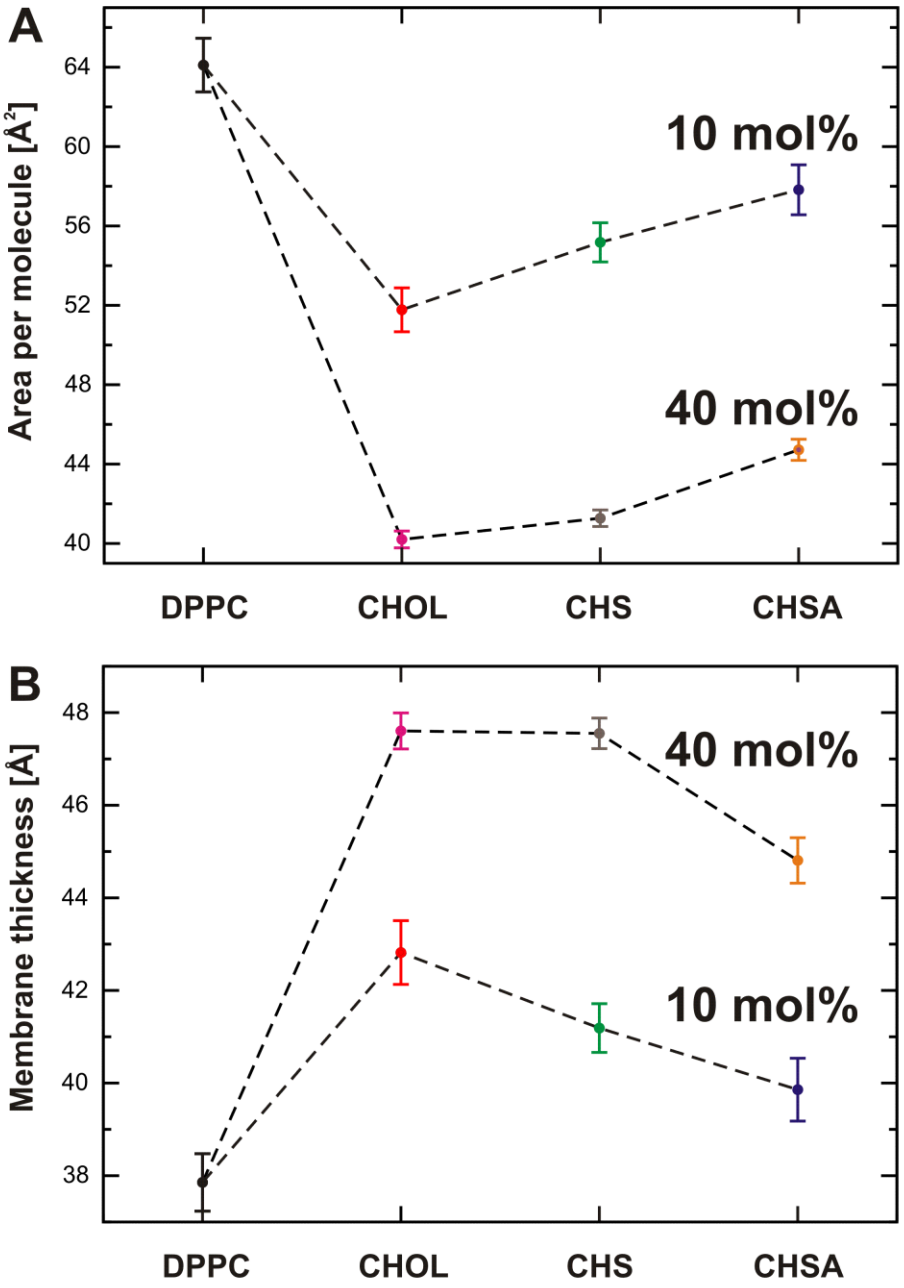
A
Area per molecule [Å²]
64
60
56
52
48
44
40
10 mol%
40 mol%
DPPC
CHOL
CHS
CHSA
B
Membrane thickness [Å]
48
46
44
42
40
38
40 mol%
10 mol%
DPPC
CHOL
CHS
CHSA

Figure 4.

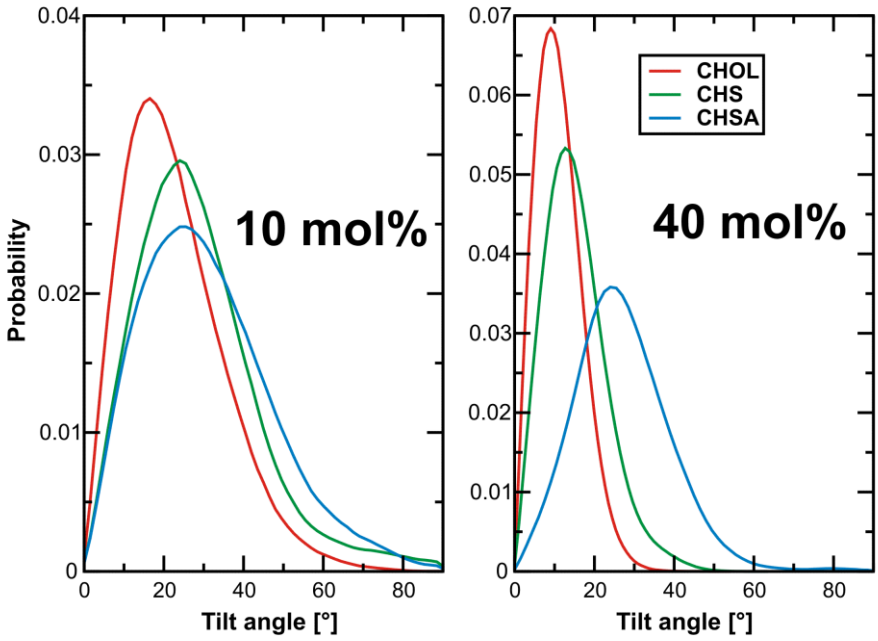
Probability
0.04
0.03
0.02
0.01
0
10 mol%
0
20
40
60
80
Tilt angle [°]
0.07
0.06
0.05
0.04
0.03
0.02
0.01
0
CHOL
CHS
CHSA
40 mol%
0
20
40
60
80
Tilt angle [°]

Figure 5.

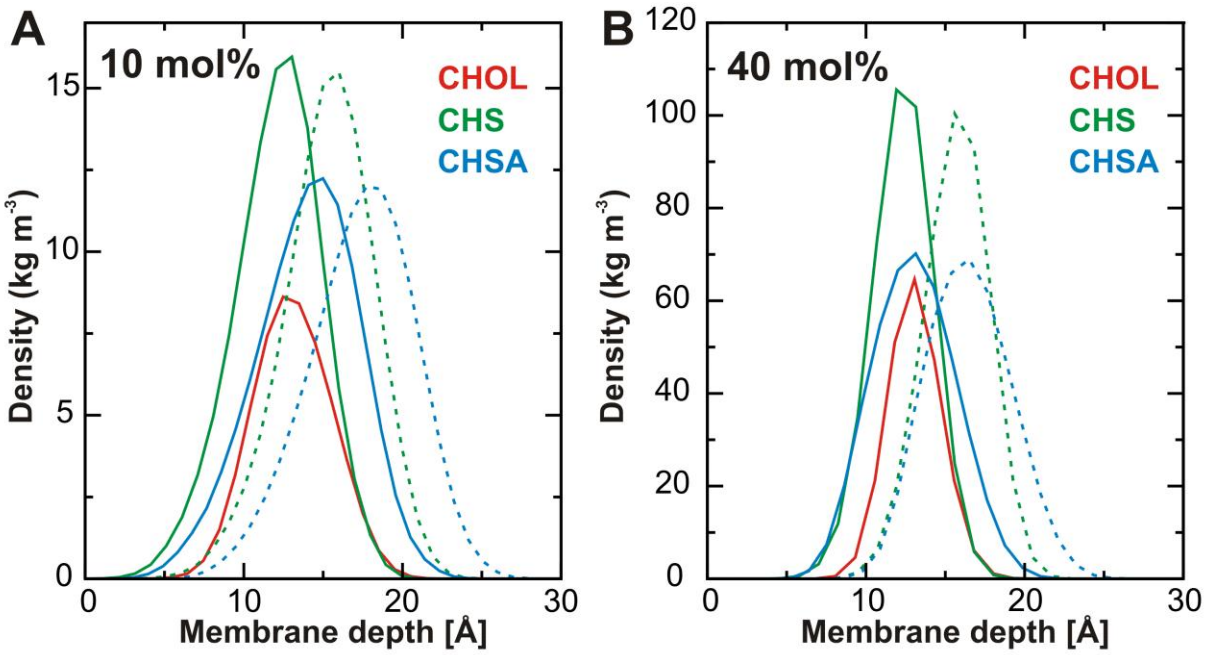
A
10 mol%
CHOL
CHS
CHSA
Density (kg m-3)
Membrane depth [Å]
B
40 mol%
CHOL
CHS
CHSA
Density (kg m-3)
Membrane depth [Å]

Figure 6.

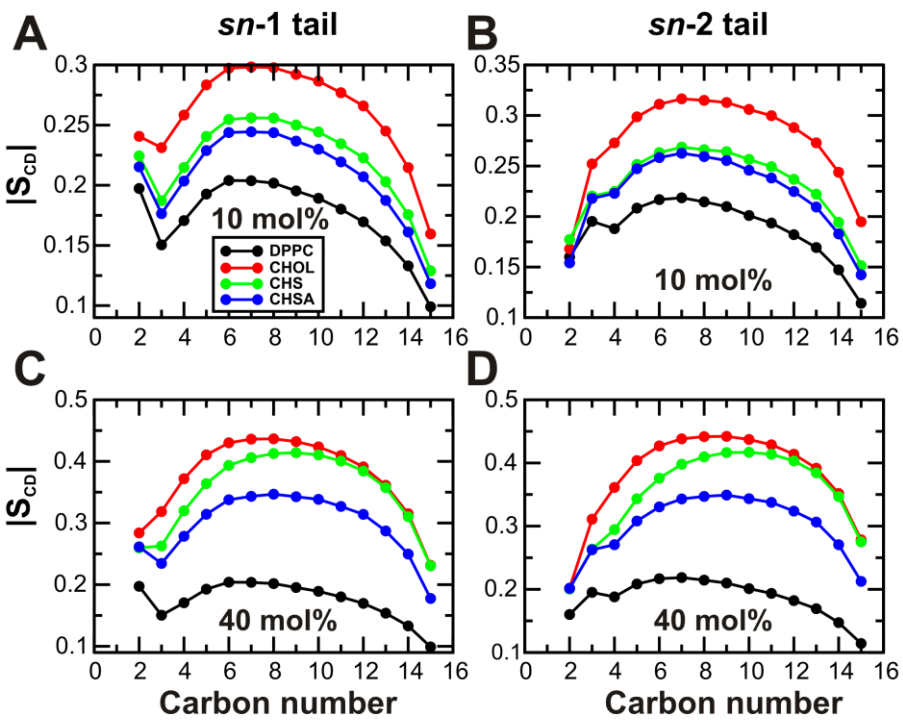
A
sn-1 tail
B
sn-2 tail
C
D
|SCD|
10 mol%
40 mol%
DPPC
CHOL
CHS
CHSA
Carbon number

Figure 7.

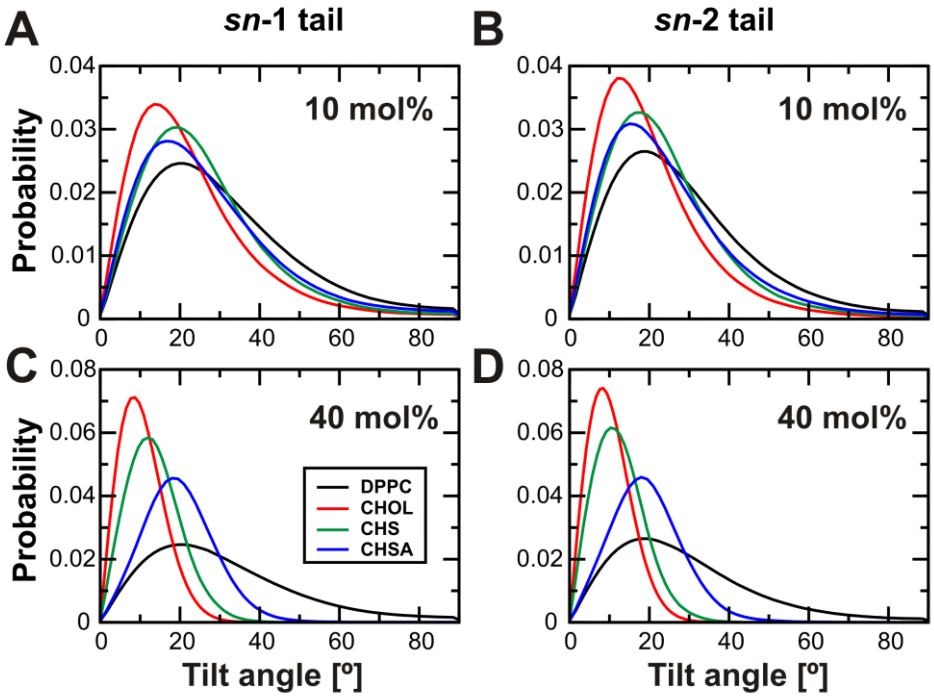
A
sn-1 tail
B
sn-2 tail
10 mol%
10 mol%
C
D
40 mol%
40 mol%
Probability
Probability
DPPC
CHOL
CHS
CHSA
Tilt angle [º]
Tilt angle [º]
0
0.01
0.02
0.03
0.04
0.06
0.08
0
20
40
60
80

Figure 8.

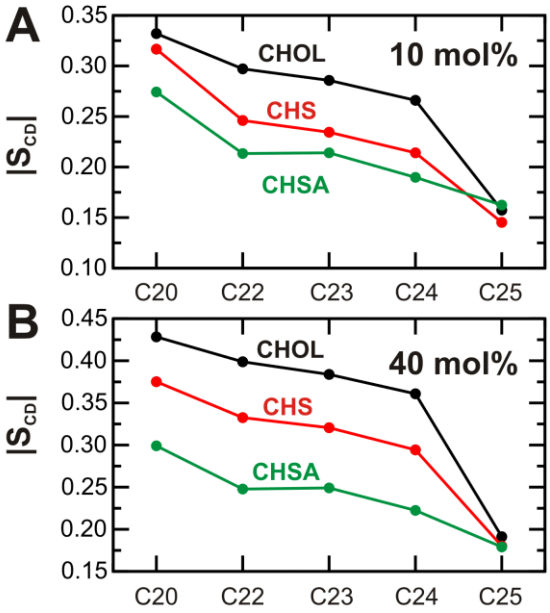
A
B
|S_CD|
CHOL
CHS
CHSA
10 mol%
40 mol%
0.35
0.30
0.25
0.20
0.15
0.10
0.45
0.40
C20
C22
C23
C24
C25

Figure 9.

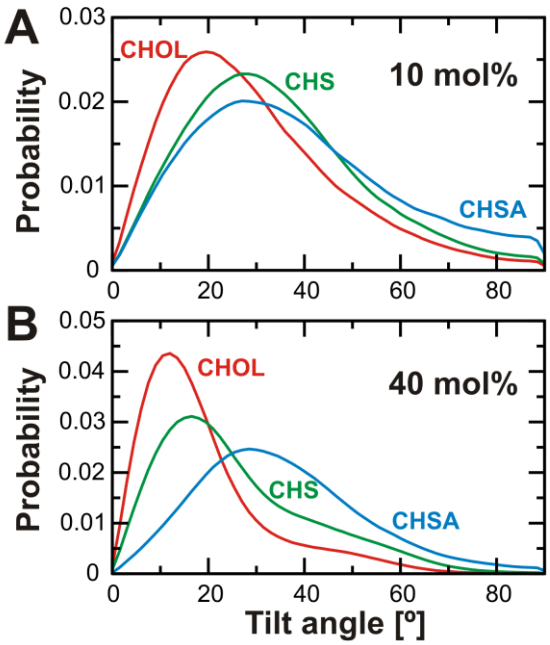
A
B
Probability
CHOL
CHS
CHSA
10 mol%
40 mol%
0.03
0.02
0.01
0
0.05
0.04
0
20
40
60
80
Tilt angle [º]

Figure 10.